Computational Materials Science 144 (2018) 315–321

Contents lists available at ScienceDirect

Computational Materials Science

journal homepage: www.elsevier.com/locate/commatsci

Density-functional theory based molecular dynamics simulation of tetrahedrite thermoelectrics: Effect of cell size and basis sets

Junchao Li, Daniel P. Weller, Donald T. Morelli, Wei Lai *

Department of Chemical Engineering and Materials Science, Michigan State University, East Lansing, MI 48824, USA

ARTICLE INFO

Article history:
Received 25 October 2017
Received in revised form 19 December 2017
Accepted 20 December 2017

Keywords:
Molecular dynamics
Tetrahedrite
Cell size
Basis set

ABSTRACT

In this work we investigated the effect of cell size and basis sets on the structural and dynamic properties from density-functional theory based molecular dynamics simulations. Three simulations, $1 \times 1 \times 1$ cell with plane wave (PW) basis set, $1 \times 1 \times 1$ cell with atomic orbital (AO) basis, and $2 \times 2 \times 2$ cell with AO basis, were performed at 300 K on a model material: tetrahedrite thermoelectric $Cu_{10}Zn_2Sb_4S_{13}$. It was found that lattice parameters, vibrational spectra, heat capacity, and EXAFS spectra are comparable for three simulations. In addition, the $2 \times 2 \times 2$ cell can provide access to length scales closer to the hydrodynamic limit, which allow us to identify the sound/acoustic modes in momentum/velocity correlation, as well as quasi-localized modes that are possibly responsible for its low lattice thermal conductivity.

1. Introduction

With the advancement of hardware and software infrastructure, computational modeling has become an indispensable tool in materials research, often in parallel with experimental effort. Among different modeling methods, density-functional theory (DFT) in the Kohn-Sham approach [1] has been widely used in the investigation of chemicals, hard materials, and soft matter. Although DFT calculations are considered as first-principles methods they are not option free, as the size of simulation cell, basis sets for the wavefunction, exchange-correlation (XC) functional, etc. must be selected first. While there are many studies on the effect of XC functionals, e.g. the recent study by Tran et al. [2], the examination of cell size is rare due to the computational overhead associated with the increase of atoms/electrons. One of the size studies by Spiekermann et al. [3] suggested different trends, e.g. water release for a 192-atom cell and water uptake for a 96-atom cell of supercritical H_2O-SiO_2 fluids, pointing to a finite size effect. In terms of basis sets, plane waves (PW) and atomic orbitals (AO) are two popular choices. Recently, Miceli et al. [4] compared the structural, dynamic, and electronic properties of liquid water using both AO and PW basis sets and found good agreement on results from two sets. Ulian et al. [5] also compared PW and AO basis sets using $Mg_3Si_4O_{10}(OH)_2$ layer silicate and found both basis sets adequately describe the geometry, energy, and infrared spectra.

Inspired by these studies, in this work we report our investigation of effect of cell size and basis set on results from DFT-based first-principles molecular dynamics simulation of a thermoelectric material: $Cu_{10}Zn_2Sb_4S_{13}$ tetrahedrite. Tetrahedrite materials with a general composition of $Cu_{12-x}M_xSb_4S_{13}$ where M is a metal dopant have emerged recently as promising thermoelectric candidates due to their elemental abundance, environmental friendliness, favorable electronic properties, and most importantly low lattice thermal conductivity (<1 $W\,m^{-1}\,K^{-1}$ for a wide temperature range) [6,7]. While this group of materials has been the subject of several DFT calculations [7–14], the effect of calculation "parameters" such as cell size and basis set remains elusive. We selected two cell sizes ($1 \times 1 \times 1$ and $2 \times 2 \times 2$) and two basis sets (PW and AO) and compared simulation results from three simulations ($1 \times 1 \times 1$ PW, $1 \times 1 \times 1$ AO, and $2 \times 2 \times 2$ AO) and with experiments.

2. Computational and experimental details

Vienna Ab initio Simulation Package (*VASP*) [15–18] code employing the Projector Augmented-Wave (PAW) method [19,20] and Quickstep code [21] implemented in cp2k [22] are employed as DFT packages using PW and AO basis sets, respectively. In *VASP*, valence electron configurations for Cu, Zn, Sb, S atoms are $4s^13d^{10}$, $4s^23d^{10}$, $5s^25p^3$, and $3s^23p^4$, respectively. The plane wave energy cutoff was 450 V. In Quickstep, the mixed Gaussian and plane wave (GPW) method, i.e. Gaussian basis sets for orbitals with auxiliary plane waves for electron density, was used. Valence electron configurations were the same as in VASP but with Godecker–Tetter–Hutter (GTH) norm-conserving pseudo potentials [23,24]. The plane wave cutoff was 1200 Ry and the atomic orbital (Gaussian) basis sets were molecular optimized double zeta-valence

* Corresponding author.
E-mail address: laiwei@msu.edu (W. Lai).

https://doi.org/10.1016/j.commatsci.2017.12.047
0927-0256/

basis sets with a polarization function (DZVP) [25]. In both cases, the generalized gradient approximation (GGA) with Perdew-Burke-Ernzerhof (PBE) parametrization [26,27] was used for the XC functional and a single Gamma point was used for the k-mesh. Two sizes of simulation cells, $1 \times 1 \times 1$ (58 atoms) and $2 \times 2 \times 2$ (464 atoms) were used based on the crystal structure of tetrahedrite (I-43 m) with Zn randomly distributed at Cu*12d* sites. We chose $1 \times 1 \times 1$ cell to compare AO and PW basis sets and AO basis set to compare $1 \times 1 \times 1$ and $2 \times 2 \times 2$ cells. Due to the exorbitant computational cost, we did not use the $2 \times 2 \times 2$ cell and PW combination.

For MD simulation, first a constant number of particles, pressure and temperature (NPT) ensemble at 300 K and zero pressure was implemented for 3 ps for $1 \times 1 \times 1$ cells in order to obtain the lattice parameters. The Langevin thermostat (friction coefficient of 50 and 1 ps^{-1} for atoms and lattice) and Parrinello and Rahman barostat (lattice mass of 10 a.m.u.) was used in *VASP*, while a Nose thermostat (time constant of 0.1 ps) and Martyna-Tuckerman-Tobias-Klein (MTTK) barostat [28] (time constant of 0.5 ps) was used in Quickstep. Next a constant number, volume, energy (NVE) ensemble was performed for 5 ps for equilibration at 300 K with velocity scaling followed by 20 ps production run. The time step was 1 fs for both NPT and NVE runs.

Synthesis of $Cu_{10}Zn_2Sb_4S_{13}$ powder was performed by mechanical alloying as described in the literature [29]. Cu K-edge X-ray absorption experiments were performed at the 4-3 beamline of Stanford Synchrotron Radiation Laboratory. We used the software SIXPack [30] to average raw data files out of three absorption scans and employed the software Athena [31] to extract the EXAFS signal.

3. Results and discussion

3.1. Average structure

Average structure of $Cu_{10}Zn_2Sb_4S_{13}$ after $1 \times 1 \times 1$ PW NVE simulation is shown in Fig. 1. Two distinct Cu sites can be identified, as Cu*12d* and Cu*12e*. Cu*12d* atoms are coordinated by four S atoms and form a tetrahedron, while Cu*12e* atoms are surrounded by three S atoms and form a triangular planar coordination. All Zn dopants were placed at Cu*12d* sites. This average structure is similar to what was observed experimentally for tetrahedrites [7,8].

3.2. Lattice parameters

Lattice parameters (a, b, c) from the NPT ensemble of $1 \times 1 \times 1$ PW and $1 \times 1 \times 1$ AO simulations at 300 K are shown in Fig. 2. It can be seen both simulations suggest a cubic structure. The average cubic lattice parameters are 10.4692 ± 0.135 Å and 10.5113 ± 0.073 Å, respectively. They are close to each other within the standard deviation. They are both higher than the literature value of 10.3833 Å [32], as the PBE XC functional tends to overestimate lattice parameters for various materials [2]. We took the lattice parameter of $2 \times 2 \times 2$ AO cell as double of $1 \times 1 \times 1$ AO cell.

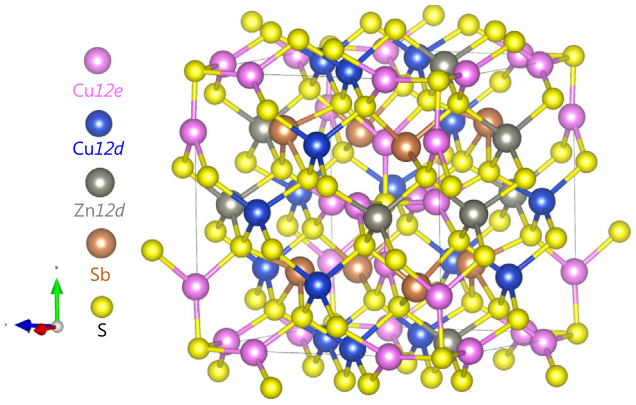

Fig. 1. Average structure after $1 \times 1 \times 1$ PW NVE simulation showing the crystal structure of $Cu_{10}Zn_2Sb_4S_{13}$.

3.3. Vibrational density of states

We investigated the effect of cell size and basis set on vibrational density of states (VDOS), which can be extracted from the atomic trajectory as the following:

$$I_{vv}(\omega) = \int_0^\infty \left\langle \frac{1}{Nk_BT} \sum_{n=1}^{N} m_n \boldsymbol{v}_n(0) \cdot \boldsymbol{v}_n(t) \right\rangle \cos(\omega t) W(t) dt \quad (1)$$

where m_n and $\boldsymbol{v}_n$ are the mass and velocity of nth atom, N the total number of atoms in the group, and $W(t)$ the Gaussian window function with a peak width of 1 meV.

The partial VDOS (a–e) of each atom group, Cu*12e*, Cu*12d*, Zn*12d*, Sb, and S and total VDOS (f) are shown in Fig. 3. The *12e* and *12d* sites are trigonal planar and tetrahedral positions, respectively. In Fig. 3a, the vibration of Cu*12e* shows three peaks (~4.2, 5.9, 7.5 eV) at the low-energy portion with the first peak being strongest for $1 \times 1 \times 1$ PW simulation, while $1 \times 1 \times 1$ AO simulation has three peaks (~4.8, 6.1, 7.8 eV) with the second and third peaks almost equal in intensity. If we compare $1 \times 1 \times 1$ AO and $2 \times 2 \times 2$ AO simulations, we can see the peak at 7.8 eV from the former decays into a shoulder in the latter. The similar observation was made for other atom groups (b-e) and the total group (f). We think that different basis sets cause slightly different electronic structures and atomic forces, leading to slight variation in vibrational properties. On the other hand, larger cells allow more atoms and vibrational modes to be sampled, which effectively broaden the peaks.

Under the harmonic approximation, the vibrational energy is connected to the total VDOS as the following:

$$U(E = \hbar\omega, T) = \int_0^\infty E/[\exp(E/(k_BT)) - 1] I_{vv}^{total}(E) dE / \int_0^\infty I_{vv}^{total}(E) dE, \quad (2)$$

from which heat capacity can be computed. The constant-volume heat capacity per atom for three simulations is shown in Fig. 4. Heat capacities of three simulations are close to each other at all temperatures and approach $3k_B$ at high temperature according to the Dulong-Petit law. In the meantime, experimental data for the same compound measured by Lara-Curzio et al. [33] and for a similar composition $Cu_{10.5}Zn_{1.5}Sb_4S_{13}$ measured by Lu et al. [7] are also shown in Fig. 4. Experimental values agree well with computed ones. It is worth noting that we assume the total VDOS (obtained from 300 K, i.e. Fig. 3f) stay the same for the entire computed range, 0–900 K.

3.4. Phonon dispersion

In addition to VDOS, we also examined the effect of cell size and basis set on phonon dispersion by comparing the Q-resolved coherent velocity correlation. For the coherent velocity, $\boldsymbol{J}(\boldsymbol{Q}, t) = \sum_{n=1}^{N} \boldsymbol{v}_n(t)$ where N is the total number of atoms, the longitudinal (L) and transverse (T) correlation can be calculated as the following:

$$C^L(Q,t) = \frac{1}{Q^2} \langle (\boldsymbol{Q} \cdot \boldsymbol{J}(\boldsymbol{Q}, 0))(\boldsymbol{Q} \cdot \boldsymbol{J}(-\boldsymbol{Q}, t)) \rangle, C^T(Q,t) = \frac{1}{2Q^2} \langle (\boldsymbol{Q} \times \boldsymbol{J}(\boldsymbol{Q}, 0)) \cdot (\boldsymbol{Q} \times \boldsymbol{J}(-\boldsymbol{Q}, t)) \rangle \quad (3)$$